


## RESEARCH ARTICLE

# Brain MRI shows white matter sparing in Kennedy's disease and slow-progressing lower motor neuron disease

Edoardo G. Spinelli<sup>1,2</sup> | Federica Agosta<sup>1</sup> | Pilar M. Ferraro<sup>1</sup> | Giorgia Querin<sup>3</sup> | Nilo Riva<sup>2</sup> | Cinzia Bertolin<sup>3</sup> | Ilaria Martinelli<sup>3</sup> | Christian Lunetta<sup>4</sup> | Andrea Fontana<sup>5</sup> | Gianni Sorarù<sup>3</sup> | Massimo Filippi<sup>1,2</sup> 

<sup>1</sup>Neuroimaging Research Unit, Institute of Experimental Neurology, Division of Neuroscience, San Raffaele Scientific Institute, Vita-Salute San Raffaele University, Milan, Italy

<sup>2</sup>Department of Neurology, Institute of Experimental Neurology, Division of Neuroscience, San Raffaele Scientific Institute, Vita-Salute San Raffaele University, Milan, Italy

<sup>3</sup>Department of Neurosciences, Neuromuscular Center, University of Padova, Padova, Italy

<sup>4</sup>NeuroMuscular Omnicentre, Fondazione Serena Onlus, Milan, Italy

<sup>5</sup>Biostatistics Unit, Fondazione IRCCS Casa Sollievo della Sofferenza, Unit of Biostatistics, Foggia, Italy

## Correspondence

Massimo Filippi, Neuroimaging Research Unit, Institute of Experimental Neurology, Division of Neuroscience, San Raffaele Scientific Institute, Vita-Salute San Raffaele University, Via Olgettina, 60, Milan 20132, Italy.  
Email: filippi.massimo@hsr.it

## Funding information

Ministero della Salute. Grant/Award Number: #RF-2010-2313220 and #RF-2011-02351193

## Abstract

The extent of central nervous system involvement in Kennedy's disease (KD) relative to other motor neuron disease (MND) phenotypes still needs to be clarified. In this study, we investigated cortical and white matter (WM) MRI alterations in 25 patients with KD, compared with 24 healthy subjects, 25 patients with sporadic amyotrophic lateral sclerosis (ALS), and 35 cases with lower motor neuron-predominant disease (LMND). LMND patients were clinically differentiated into 24 fast and 11 slow progressors. Whole-brain cortical thickness, WM tract-based spatial statistics and corticospinal tract (CST) tractography analyses were performed. No significant difference in terms of cortical thickness was found between groups. ALS patients showed widespread decreased fractional anisotropy and increased mean (MD) and radial diffusivity (radD) in the CST, corpus callosum and fronto-temporal extra-motor tracts, compared with healthy controls and other patient groups. CST tractography showed significant alterations of DT MRI metrics in ALS and LMND-fast patients whereas KD and LMND-slow patients were comparable with healthy controls. Our study demonstrated the absence of WM abnormalities in patients with KD and LMND-slow, in contrast with diffuse WM damage in ALS and focal CST degeneration in LMND-fast, supporting the use of DT MRI measures as powerful tools to differentiate fast- and slow-progressing MND syndromes, including KD.

## KEYWORDS

amyotrophic lateral sclerosis, corticospinal tract, diffusion tensor MRI, Kennedy's disease, lower motor neuron disease

## 1 | INTRODUCTION

Kennedy's disease (KD) is an X-linked neurodegenerative disease of the motor neurons caused by a CAG repeat expansion within the first exon of the androgen receptor gene (La Spada, Wilson, Lubahn, Harding, & Fischbeck, 1991; Lee et al., 2005). The clinical picture is dominated by lower motor neuron (LMN) signs, including progressive muscle wasting, fasciculations, and reduced deep tendon reflexes

(Grunseich, Rinaldi, & Fischbeck, 2014). Among motor neuron diseases (MND), KD shows slow disease progression and normal or minimally reduced life expectancy (Chahin, Klein, Mandrekar, & Sorenson, 2008). However, the mean diagnostic delay of this condition is 5.5 years (Finsterer, 2010; Rhodes et al., 2009), as KD patients are often initially misdiagnosed as amyotrophic lateral sclerosis (ALS). Therefore, the identification of noninvasive biomarkers differentiating KD from classic MND phenotypes is of crucial prognostic relevance.

Only a few previous magnetic resonance imaging (MRI) studies investigated central nervous system (CNS) involvement in KD patients, showing white matter (WM) alterations mainly involving the corticospinal tracts (CST) and frontal subcortical areas, as well as subtle atrophy in frontal gray matter (GM) regions (Garaci et al., 2015; Kassubek, Juengling, & Sperfeld, 2007; Pieper, Konrad, Sommer, Teismann, & Schiffbauer, 2013; Unrath et al., 2010). However, previous studies have focused on structural alterations in KD relative to healthy controls, while the extent of CNS involvement relative to other MND phenotypes still needs further clarification. Particularly, WM alterations have been suggested to help in differentiating LMN-predominant disease (LMND) with faster and slower progression, as the former might represent early ALS cases (Muller et al., 2018). Evaluating where KD cases fall within this wide range of CNS alterations has clear clinical implications.

Therefore, the aim of this multiparametric MRI study was to investigate cerebral damage in a sizeable sample of KD patients relative to healthy controls and MND patients with classic ALS and LMND.

## 2 | METHODS

This prospective study was approved by the Local Ethical Committee on human studies and written informed consent from all subjects (or their legal guardians) was obtained prior to their enrollment.

### 2.1 | Subjects

All patients were consecutively recruited from three tertiary referral MND clinics in Northern Italy between October 2009 and April 2016. Twenty-five patients with genetically confirmed KD were included (Table 1). Two additional sets of 25 patients with sporadic possible, probable, or definite ALS (Brooks, Miller, Swash, Munsat, & World Federation of Neurology Research Group on Motor Neuron, 2000)

showing signs of both UMN and LMN involvement and 35 patients with a clinical diagnosis of sporadic LMND (Chio et al., 2011; van den Berg-Vos et al., 2003) were enrolled to match KD patients for disease severity, as assessed using the revised version of ALS Functional Rating Scale (ALSFRS-r; Table 1). The diagnosis of LMND was based on the presence of pure LMN findings in two or more regions (bulbar, cervical, thoracic, lumbosacral) at the clinical evaluation, including evidence of LMN involvement on neurological examination (weakness and muscular atrophy, absent tendon reflexes), electrophysiological evidence of LMN involvement on standardized needle EMG, and no motor nerve conduction block. Patients with LMND were divided into fast and slow progressors, using a disease duration of 4 years as the timepoint to discriminate the two subtypes, as previously suggested (Rosenbohm, Muller, Hubers, Ludolph, & Kassubek, 2016; van den Berg-Vos et al., 2003). As a result, 24 LMND-fast and 11 LMND-slow patients were identified. All patients underwent a comprehensive evaluation including neurological examination, neuropsychological and behavioral evaluations, and MRI scan. Experienced neurologists blinded to the MRI results performed the clinical assessment. Disease duration was recorded. The rate of disease progression was calculated as 48 minus the ALS Functional Rating Score divided by time in months from symptom onset, as previously described (Ciccarelli et al., 2006). In KD patients, functional capacity was evaluated using the 6-min walk test, and body mass index (BMI) was calculated as follows: weight (kg)/height<sup>2</sup> (m<sup>2</sup>).

Comprehensive neuropsychological and behavioral evaluations were performed by a trained neuropsychologist unaware of the MRI results, assessing: global cognitive functioning with the Mini-Mental State Examination (MMSE) (Folstein, Folstein, & McHugh, 1975); reasoning and executive functions with the Raven colored progressive matrices (Basso, Capitani, & Laiacina, 1987), phonemic and semantic fluency tests (Novelli et al., 1986), digit span backward (Monaco, Costa, Caltagirone, & Carlesimo, 2013), Cognitive Estimation Task, (Della Sala, MacPherson, Phillips, Sacco, & Spinnler, 2003), Wisconsin

**TABLE 1** Demographic and clinical findings of healthy controls, KD, ALS, and LMND patients

	Healthy controls	KD	ALS	LMND-fast	LMND-slow	<i>p</i> *
Number	24	25	25	24	11	
Age (years)	58.5 ± 5.7	57.0 ± 6.5 <sup>c</sup>	61.5 ± 9.7 <sup>b</sup>	60.8 ± 8.5	56.4 ± 7.9	.11
Sex (W/M)	10/14 <sup>b</sup>	0/25 <sup>a,c,d,e</sup>	10/15 <sup>b</sup>	8/16 <sup>b</sup>	4/7 <sup>b</sup>	.007
Education (years)	14.7 ± 4.6 <sup>b,c,d</sup>	11.0 ± 3.2 <sup>a</sup>	10.3 ± 3.8 <sup>a</sup>	10.8 ± 5.3 <sup>a</sup>	12.8 ± 3.1	.003
Disease duration (months)	-	144.6 ± 63.9 <sup>c,d</sup>	21.8 ± 21.0 <sup>b,e</sup>	17.5 ± 9.3 <sup>b,e</sup>	146.8 ± 123 <sup>c,d</sup>	<.001
ALSFRS-R (0–48)	-	41.3 ± 3.6	39.7 ± 6.1	39.1 ± 6.1	38.8 ± 7.9	.67
Disease progression rate (ALSFRS-R rate of decline per month)	-	0.05 ± 0.02 <sup>c,d</sup>	0.68 ± 0.72 <sup>b,e</sup>	0.66 ± 0.61 <sup>b,e</sup>	0.09 ± 0.10 <sup>c,d</sup>	<.001
6MWT (meters)	-	330.7 ± 98.8	-	-	-	-
BMI (kg/m <sup>2</sup> )	-	26.5 ± 3.0	-	-	-	-
Number of CAG repeats	-	45.1 ± 5.5	-	-	-	-

Values are means ± standard deviations. \**P* values refer to Pearson Chi-Square or ANOVA models, followed by post-hoc pairwise comparisons.

a = *p* < 0.05 vs. HC; b = *p* < 0.05 vs. KD; c = *p* < 0.05 vs. classic ALS; d = *p* < 0.05 vs. LMND-fast; e = *p* < 0.05 vs. LMND-slow at posthoc pairwise comparisons. Abbreviations. 6MWT: six-minute walk test; ALS: amyotrophic lateral sclerosis; ALSFRS-R: ALS functional rating scale-revised; BMI: body mass index; KD: Kennedy's disease; LMND: lower motor neuron-predominant disease; M: men; W: women.

Card Sorting Test (WCST; Laiacona, Inzaghi, De Tanti, & Capitani, 2000), and Weigl's Sorting Test (Weigl, 1927); verbal memory with the digit span forward (Orsini et al., 1987) and the Rey Auditory Verbal Learning Test (RAVLT) immediate and delayed recall (Carlesimo, Caltagirone, & Gainotti, 1996); and language with the oral noun confrontation naming subtest of BADA (Batteria per l'Analisi dei Deficit Afasici; Miceli, Laudanna, Burani, & Capasso, 1994). Depressive symptoms were assessed using the Hamilton Depression Rating Scale (Hamilton, 1960). Behavioral disturbances were determined based on direct observation and patient's history, caregiver report, the Frontal Behavioral Inventory (Alberici et al., 2007) and the ALS-FTD questionnaire (Raaphorst et al., 2012), which were administered to the patients' caregiver. Patient cognitive and behavioral profiles were classified according to the revised Strong criteria for cognitive impairment in ALS (Strong et al., 2017).

Twenty-four age-matched healthy controls were recruited among spouses of patients and by word of mouth (Table 1). Healthy controls were included if neurological examination was normal and MMSE was  $\geq 28$ . Exclusion criteria of the present study were: dementia or frontotemporal lobar degeneration (FTLD)-related disorders; significant medical illnesses or substance abuse that could interfere with cognitive functioning; any (other) major systemic, psychiatric, or neurological illness; and other causes of focal or diffuse brain damage, including lacunae and extensive cerebrovascular disorder at MRI. ALS and LMND patients were also excluded if they had a family history of MND.

## 2.2 | MRI acquisition

For the MRI scan, the heads of the subjects were positioned carefully with restraining foam pads to reduce head motion, and ear plugs were used to reduce scanner noise. A strap was also positioned around the head to provide additional stabilization. Using a 3.0 T scanner (Intera, Philips Medical Systems, Best, the Netherlands), the following brain MRI sequences were obtained from all subjects: T2-weighted spin echo (SE; repetition time [TR] = 3,500 ms; echo time [TE] = 85 ms; echo train length = 15; flip angle =  $90^\circ$ ; 22 contiguous, 5-mm-thick, axial slices; matrix size =  $512 \times 512$ ; field of view [FOV] =  $230 \times 184 \text{ mm}^2$ ); fluid-attenuated inversion recovery (TR = 11 s; TE = 120 ms; flip angle =  $90^\circ$ ; 22 contiguous, 5-mm-thick, axial slices; matrix size =  $512 \times 512$ ; FOV =  $230 \text{ mm}^2$ ); 3D T1-weighted fast field echo (FFE) (TR = 25 ms, TE = 4.6 ms, flip angle =  $30^\circ$ , 220 contiguous axial slices with voxel size =  $0.89 \times 0.89 \times 0.8 \text{ mm}$ , matrix size =  $256 \times 256$ , FOV =  $230 \times 182 \text{ mm}^2$ ); and pulsed-gradient SE echo planar with sensitivity encoding (acceleration factor = 2.5, TR = 8,986 ms, TE = 80 ms, 55 contiguous, 2.5 mm-thick axial slices, number of acquisitions = 2; acquisition matrix  $96 \times 96$ , with an in-plane pixel size of  $1.89 \times 1.89 \text{ mm}$  and a FOV =  $240 \text{ mm}^2$ ) diffusion gradients applied in 32 noncollinear directions using a gradient scheme which is standard on this system (gradient over-plus) and optimized to reduce echo time as much as possible. The *b* factor used was  $1,000 \text{ s/mm}^2$ . Fat saturation was performed to avoid chemical shift artifacts. All slices were positioned to run

parallel to a line that joins the most inferoanterior and inferoposterior parts of the corpus callosum.

## 2.3 | MRI analysis

### 2.3.1 | Cortical thickness measurement

Cortical reconstruction and estimation of cortical thickness were performed on the 3D T1-weighted FFE images using the FreeSurfer image analysis suite, version 5.3 (<http://surfer.nmr.mgh.harvard.edu/>), by a single observer blinded to patients' identity. After registration to Talairach space and intensity normalization, the process involved an automatic skull stripping, which removes extra-cerebral structures, cerebellum and brainstem, by using a hybrid method combining watershed algorithms and deformable surface models. Images were then carefully checked for skull stripping errors. After this step, images were segmented into GM, WM, and cerebrospinal fluid (CSF), cerebral hemispheres were separated, and subcortical structures divided from cortical components. The WM/GM boundary was tessellated, and the surface was deformed following intensity gradients to optimally place WM/GM and GM/CSF borders, thus obtaining the WM and pial surfaces (Dale, Fischl, & Sereno, 1999). The results of this segmentation procedure were inspected visually, and if necessary, edited manually by adding control points. Afterward, surface inflation and registration to a spherical atlas were performed (Dale et al., 1999). Finally, cortical thickness was estimated as the average shortest distance between the WM boundary and the pial surface.

### 2.3.2 | Diffusion tensor (DT) MRI analysis

DT MRI analysis was performed using the FMRIB software library (FSL) tools (<http://www.fmrib.ox.ac.uk/fsl/fdt/index.html>) and the JIM5 software (Xinapse Systems, Northants, UK, <http://www.xinapse.com>), as previously described (Agosta et al., 2013, 2014). The diffusion-weighted data underwent a careful quality check for head motion and were subsequently skull-stripped using the Brain Extraction Tool implemented in FSL. Using FMRIB's Linear Image Registration Tool (FLIRT), the two diffusion-weighted scans were coregistered by applying the rigid transformation needed to correct for position between the two *b*<sub>0</sub> images (T2-weighted, but not diffusion-weighted). The rotation component was also applied to diffusion-weighted directions. Eddy currents correction was performed using JIM5 (Horsfield, 1999). The DT was estimated on a voxel-by-voxel basis using DTifit provided by the FMRIB Diffusion Toolbox. Maps of fractional anisotropy (FA), mean diffusivity (MD), axial diffusivity (axD), and radial diffusivity (radD) were obtained.

Firstly, a whole-brain DT MRI analysis was performed using tract-based spatial statistics (TBSS) version 1.2 (<http://www.fmrib.ox.ac.uk/fsl/tbss/index.html>). Secondly, fiber tracking of the CST bilaterally was performed. For TBSS analysis, FA volumes were aligned to a target image using the following procedure: (a) the FA template in standard space (provided by FSL) was selected as the target image, (b) the nonlinear transformation that mapped each subject's FA to the target

image was computed using the FMRIB's Nonlinear Image Registration Tool, and (c) the same transformation was used to align each subject's FA to the standard space. A mean FA image was then created by averaging the aligned individual FA images and thinned to create a FA skeleton representing WM tracts common to all subjects. The FA skeleton was thresholded at a value of 0.2 to exclude voxels with low FA values, which are likely to include GM or CSF. Individual FA, MD, axD, and radD data were projected onto this common skeleton. Seeds for tractography of the CST were drawn at the top of bulbar pyramids in the Montreal Neurological Institute (MNI) space on the FA template provided by FSL and included four axial slices, as previously described (Agosta et al., 2013, 2014). Fiber tracking was performed in the native DT MRI space using a probabilistic tractography algorithm implemented in FSL (probtrackx), which is based on Bayesian estimation of diffusion parameters (Bedpostx) (Behrens, Berg, Jbabdi, Rushworth, & Woolrich, 2007). Fiber tracking was initiated from all voxels within the seed masks in the diffusion space to generate 5,000 streamline samples with a step length of 0.5 mm and a curvature threshold of 0.2. Using a "single-seed" approach, the reconstruction of the CST was obtained, bilaterally. Tract maps were then normalized taking into consideration the number of voxels in the seed masks. To do so, the number of streamline samples present in the voxels of the tract maps was divided by the way-total, which corresponds to the total number of streamline samples that were not rejected by the exclusion masks. The tract masks obtained were thresholded at a value equal to 40% of the 95th percentile of the distribution of the intensity values of the voxels included in the tract, as previously described (Galantucci et al., 2011). This normalization procedure allowed us to correct for possible differences between tracts due to the different sizes of the starting seeds. In this way, we also excluded the background noise and avoided a too restrictive thresholding when the maximum intensity value was an outlier. Group probability maps of each thresholded tract (i.e., left and right CST) were produced to visually check their anatomical consistency across study subjects (see Supporting Information Figure S1). For each subject, the average FA, MD, axD, and radD of the CST were calculated in the native space.

## 2.4 | Statistical analysis

Group comparisons of demographic, clinical, cognitive, and CST tractography data were performed using analysis of covariance (ANCOVA) models followed by posthoc pairwise comparisons, adjusting for subjects' age and sex and controlling the False Discovery Rate (FDR) at level .05, using Benjamini-Hochberg step-up procedure. For the analysis of CST tractography data,  $p$  values from ANCOVA  $F$ -tests were also bootstrapped, as described by Westfall & Young (1993). Briefly, the bootstrap procedure consisted of the following steps: (a) a full ANCOVA model (which included the intercept and age, sex, and subject group as covariates) was fitted and the observed  $F$ -values were obtained; (b) a null model (including the intercept with age and sex as covariates) was fitted using those observations previously considered in the full model and residuals were retrieved; (c) such residuals were centered and rescaled by leverage values;

(d) subsequently, a new dependent variable for bootstrapping was built as the sum of the fitted values of the null model and the resampled residuals estimated from the same null model; (e) finally, a new "bootstrapped" full ANCOVA model was fitted using the calculated dependent variable and an  $F$ -sample was obtained. The last two steps were repeated 1,000 times. The bootstrapped  $p$  value was determined as the proportion of resampled  $F$ -values that are greater than the observed  $F$ -values. Two-sided  $p$  values  $<.05$  were considered for statistical significance.

A vertex-by-vertex analysis was used to assess differences of cortical thickness between groups using a general linear model in FreeSurfer. Statistical maps were thresholded at  $p <.05$ , using the FDR correction for multiple comparisons, adjusting for age and sex. Regarding the TBSS analysis, DT MRI voxelwise statistics were performed using a permutation-based inference tool for nonparametric statistical thresholding ("randomize," part of FSL) (Nichols & Holmes, 2002). FA, MD, axD, and radD values within the skeleton were compared between groups using permutation-based two-sample  $t$  tests, adjusting for age and sex. The number of permutations was set at 5,000. Statistical maps were thresholded at  $p <.05$ , family-wise error (FWE) corrected for multiple comparisons at the cluster level using the threshold-free cluster enhancement (TFCE) option (Smith & Nichols, 2009).

## 3 | RESULTS

### 3.1 | Demographic, clinical, and cognitive features

Patient groups were well-matched in terms of disease severity ( $p = 0.67$ ) (Table 1). As expected, KD patients were younger than classic ALS patients ( $p = .05$ ). KD and LMND-slow patients had longer disease duration ( $p < 0.001$ ) and slower disease progression ( $p < 0.001$ ) relative to classic ALS and LMND-fast cases (Table 1).

The neuropsychological features of KD, ALS, and LMND patients are shown in Table 2. According to the revised Strong criteria (Strong et al., 2017), 36% of KD, 43% of ALS, 39% of LMND-fast, and 30% of LMND-slow patients had some degree of cognitive or behavioral impairment. Among KD patients, 20% showed isolated behavioral impairment (MND-bi) and 16% had a combined cognitive and behavioral impairment (MND-cbi). Among ALS patients, cognitive impairment (MND-ci) was found in 29% of patients, and MND-bi in 14% of cases. Among LMND-fast cases, 28% showed MND-ci, and 11% had MND-bi. Among LMND-slow, 20% of patients had MND-ci and 10% showed MND-bi. When cognitive scores were compared between groups, we found significant greater executive impairment shown by global WCST scores in ALS relative to KD patients (Table 2,  $p = .04$ ). No significant differences in other cognitive measures were found between groups.

### 3.2 | MRI findings

#### 3.2.1 | Cortical thickness

Vertex-wise analysis did not show any significant difference between groups in terms of cortical thickness (using FDR correction).

**TABLE 2** Neuropsychological and behavioral features of KD, classic ALS, and LMND patients

	KD	ALS	LMND-fast	LMND-slow	<i>p</i> *
<i>General cognition</i>					
MMSE (normal $\geq 24$ )	29.1 $\pm$ 1.3	27.8 $\pm$ 2.5	28.1 $\pm$ 2.6	28.7 $\pm$ 1.2	.36
<i>Reasoning and executive functions</i>					
Raven's colored progressive matrices (normal $\geq 18$ )	31.5 $\pm$ 3.5	28.3 $\pm$ 5.9	27.3 $\pm$ 7.9	30.3 $\pm$ 6.5	.61
Phonemic fluency (normal $\geq 17$ )	32.5 $\pm$ 9.3	27.3 $\pm$ 8.5	30.5 $\pm$ 13.0	30.8 $\pm$ 9.9	.55
Semantic fluency (normal $\geq 25$ )	45.5 $\pm$ 9.1	39.5 $\pm$ 11.6	38.6 $\pm$ 11.3	41.2 $\pm$ 10.5	.40
Digit span backward (normal $\geq 3.29$ )	4.7 $\pm$ 1.0	4.3 $\pm$ 1.4	4.1 $\pm$ 0.8	4.3 $\pm$ 1.0	.71
CET (normal $\leq 18$ )	12.9 $\pm$ 2.8	12.4 $\pm$ 3.0	14.7 $\pm$ 5.0	13.2 $\pm$ 3.7	.47
WCST (normal $\leq 90.5$ )	37.9 $\pm$ 33.6 <sup>a</sup>	96.6 $\pm$ 43.8 <sup>b</sup>	68.6 $\pm$ 43.5	62.1 $\pm$ 38.1	.04
Weigl's sorting test (normal $\geq 4.50$ )	12.3 $\pm$ 2.6	10.6 $\pm$ 4.3	13.0 $\pm$ 5.7	11.7 $\pm$ 3.9	.60
<i>Verbal memory</i>					
Digit span forward (normal $\geq 3.75$ )	5.8 $\pm$ 0.9	5.8 $\pm$ 1.3	5.5 $\pm$ 0.9	6.1 $\pm$ 0.6	.51
RAVLT, immediate recall (normal $\geq 28.53$ )	43.4 $\pm$ 10.0	38.6 $\pm$ 12.5	39.9 $\pm$ 12.0	46.3 $\pm$ 10.7	.56
RAVLT, delayed recall (normal $\geq 4.69$ )	8.8 $\pm$ 2.9	8.6 $\pm$ 3.8	7.0 $\pm$ 3.1	8.4 $\pm$ 3.7	.28
<i>Language</i>					
Oral noun confrontation naming subtest of BADA (normal $\geq 28$ )	29.6 $\pm$ 1.0	28.8 $\pm$ 1.6	29.4 $\pm$ 0.9	29.4 $\pm$ 1.0	.23
<i>Behavioral disturbances</i>					
FBI	7.5 $\pm$ 5.0	3.3 $\pm$ 6.5	2.7 $\pm$ 3.7	3.8 $\pm$ 6.9	.31
ALS-FTD questionnaire (normal $\leq 22$ )	16.7 $\pm$ 13.7	2.5 $\pm$ 5.0	11.1 $\pm$ 17.4	12.5 $\pm$ 27.0	.49
<i>Depression</i>					
HDRS (normal $\leq 9$ )	3.7 $\pm$ 2.3	3.9 $\pm$ 3.9	3.9 $\pm$ 2.4	4.4 $\pm$ 3.1	.79

Values are means  $\pm$  standard deviations. \**P* values refer to ANCOVA models adjusted for subjects' age and sex, followed by post-hoc pairwise comparisons. a =  $p < 0.05$  vs. classic ALS; b =  $p < 0.05$  vs. KD; Abbreviations: ALS = Amyotrophic lateral sclerosis; ALS-FTD = Amyotrophic lateral sclerosis-frontotemporal dementia; CET = Cognitive Estimation Test; FBI = Frontal behavioral inventory; HC = healthy controls; HDRS = Hamilton Depression Rating Scale; KD = Kennedy's disease; LMND = lower motor neuron-predominant disease; MMSE = Mini Mental State Examination; RAVLT = Rey Auditory Verbal Learning Test; WCST = Wisconsin Card Sorting Test.

### 3.2.2 | TBSS

Compared with healthy controls, the voxel-wise analysis showed no significant alterations of DT MRI metrics in KD, LMND-fast, and LMND-slow patients. Conversely, ALS patients showed a widespread pattern of increased MD and radD and decreased FA including the whole CST, genu, mid-body, and splenium of the corpus callosum, anterior limb of the internal capsule, superior longitudinal fasciculus (SLF), temporal portions of the inferior longitudinal fasciculus (ILF), and thalamic radiations bilaterally compared with healthy controls ( $p < .05$  FWE, Figure 1). Compared with KD patients, ALS patients had a pattern of FA reduction and MD and radD increase similar to that shown relative to controls ( $p < .05$  FWE, Figure 2). A widespread pattern of FA decrease and MD and radD increase encompassing the CST, corpus callosum, frontal, and parietal WM projections was also shown when ALS patients were compared with LMND-fast patients ( $p < .05$  FWE, Figure 3a). A similar pattern of FA decrease and radD increase, although more centered upon the CST, corpus callosum, and the SLF, was found when ALS patients were compared with the smallest group of LMND-slow patients ( $p < .05$  FWE, Figure 3b). The voxel-wise analysis did not show any significant difference in terms of DT MRI metrics when comparing KD, LMND-fast, and LMND-slow patients, even pooling the last two groups into one LMND group.

### 3.2.3 | CST tractography

Compared with healthy controls, tractography analysis showed no alterations of DT MRI metrics of the CST in KD and LMND-slow patients (Table 3, Figure 4). By contrast, both ALS and LMND-fast patients showed increased MD and radD values of the right CST compared with healthy controls (Table 3, Figure 4). No significant difference in FA and axD values of the CST was detected between groups.

## 4 | DISCUSSION

To date, this is the largest multiparametric MRI study performed in patients with KD, as well as the first assessing a direct comparison with other MND presentations, including LMND. In the present cohort, no significant structural alterations of the cerebral cortex and WM regions were demonstrated in KD patients compared with healthy controls. By contrast, classic ALS patients showed an extensive degeneration of both motor and extra-motor WM regions compared with healthy controls and all other MND phenotypes, including KD. To a lesser degree, also the other relatively fast-progressing MND group (i.e., LMND-fast) showed relevant damage of the CST, whereas



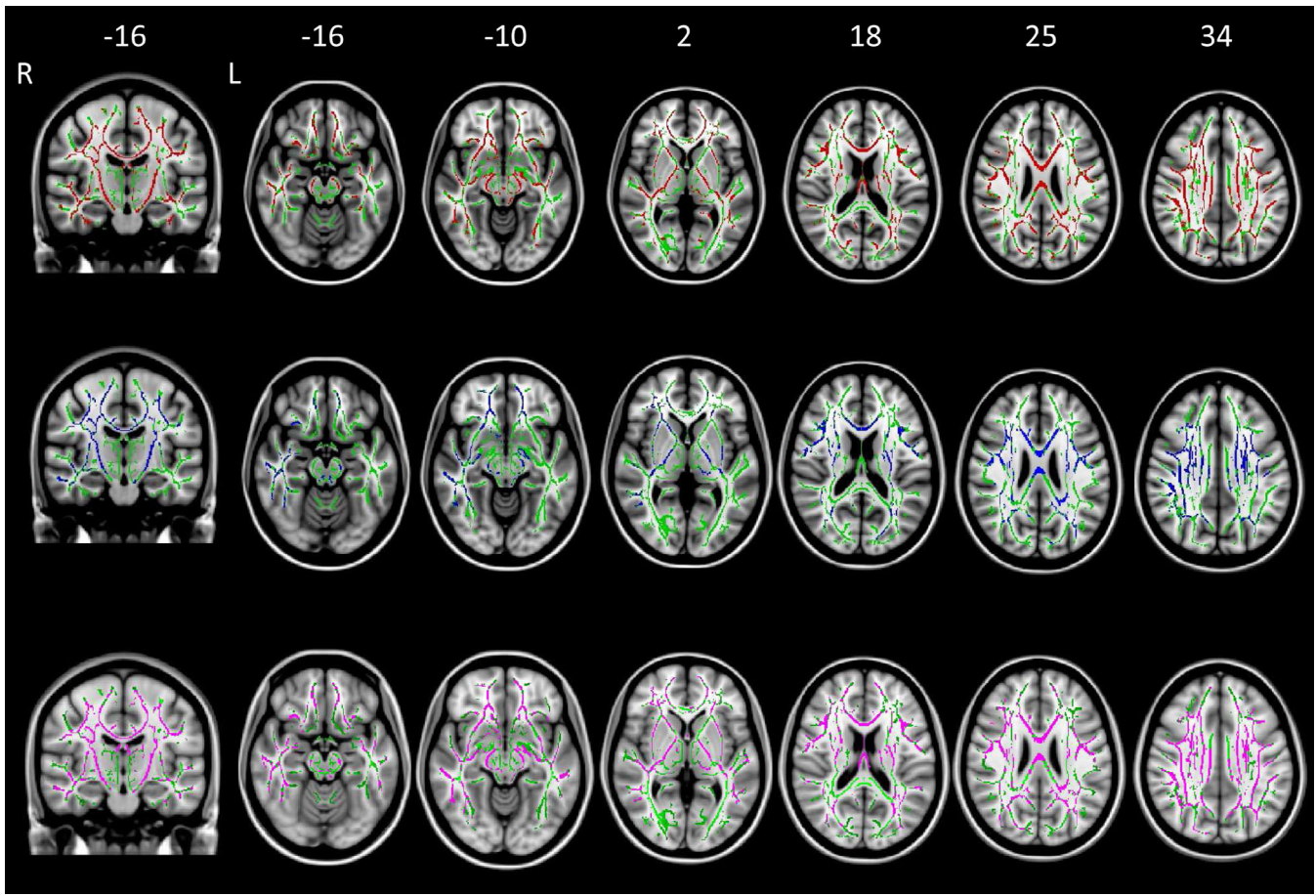


**FIGURE 1** TBSS results of comparison between classic ALS patients and healthy controls. Axial and coronal T1-weighted images of the Montreal Neurologic Institute standard brain show tract-based spatial statistics (TBSS) results in patients with classic ALS compared with healthy control subjects. Voxel-wise group differences in fractional anisotropy (red), mean diffusivity (blue), and radial diffusivity (purple) are shown. Results were overlaid on white-matter skeleton images (green;  $p < .05$ , corrected for multiple comparisons). Abbreviations. ALS: amyotrophic lateral sclerosis; L: left; R: right [Color figure can be viewed at [wileyonlinelibrary.com](http://wileyonlinelibrary.com)]

LMND-slow cases had no structural alterations compared with healthy controls and KD patients.

The distributed involvement of motor and extra-motor WM regions in our ALS cohort is largely consistent with previous literature (Agosta et al., 2014; Chio et al., 2014; Spinelli et al., 2016). The absence of significant WM alterations in KD patients is also in line with previous observations in slow-progressing MND phenotypes with predominant LMN involvement (Muller et al., 2018; Spinelli et al., 2016) and confirms the role of DT MRI metrics as promising markers of upper motor neuron (UMN) damage. Of note, the presence of CST alterations in both the ALS and LMND-fast groups suggests that DT MRI is highly sensitive to UMN degeneration below the clinical threshold of detection, possibly even indicating those LMND cases which might represent early ALS presentations (Muller et al., 2018). It is noteworthy that some prior MRI studies have reported WM changes in KD, mainly encompassing frontal regions, as well as the limbic system and CST (Kassubek et al., 2007; Unrath et al., 2010). One possible explanation for the discrepancy among results might be the shorter disease duration of patients here included (i.e., ~12 years

compared with 22–24 years of other cohorts). Relative to previous MRI studies (Kassubek et al., 2007; Unrath et al., 2010), KD patients in our cohort were indeed in an earlier phase of the disease, and this might contribute to explain the lack of significant WM damage. The only study assessing DT MRI of KD patients with a disease duration similar to the present cohort actually could not detect significant WM alterations when applying correction for multiple comparisons (Pieper et al., 2013), as we did. Accordingly, one previous MRI study has reported a significant correlation between longer disease duration and WM damage encompassing the corpus callosum, association fibers and midbrain in KD (Garaci et al., 2015), suggesting that WM alterations might be a late phenomenon in the disease course.

In the present study, we could not detect significant GM atrophy in any of the included MND groups, compared with healthy controls. The absence of GM atrophy in KD accompanies the lack of WM microstructural damage in our cohort. This finding is in contrast with one previous voxel-based morphometry study reporting GM atrophy in frontal cortical regions of KD patients (Kassubek et al., 2007), but this difference likely derives from the different MRI technique here

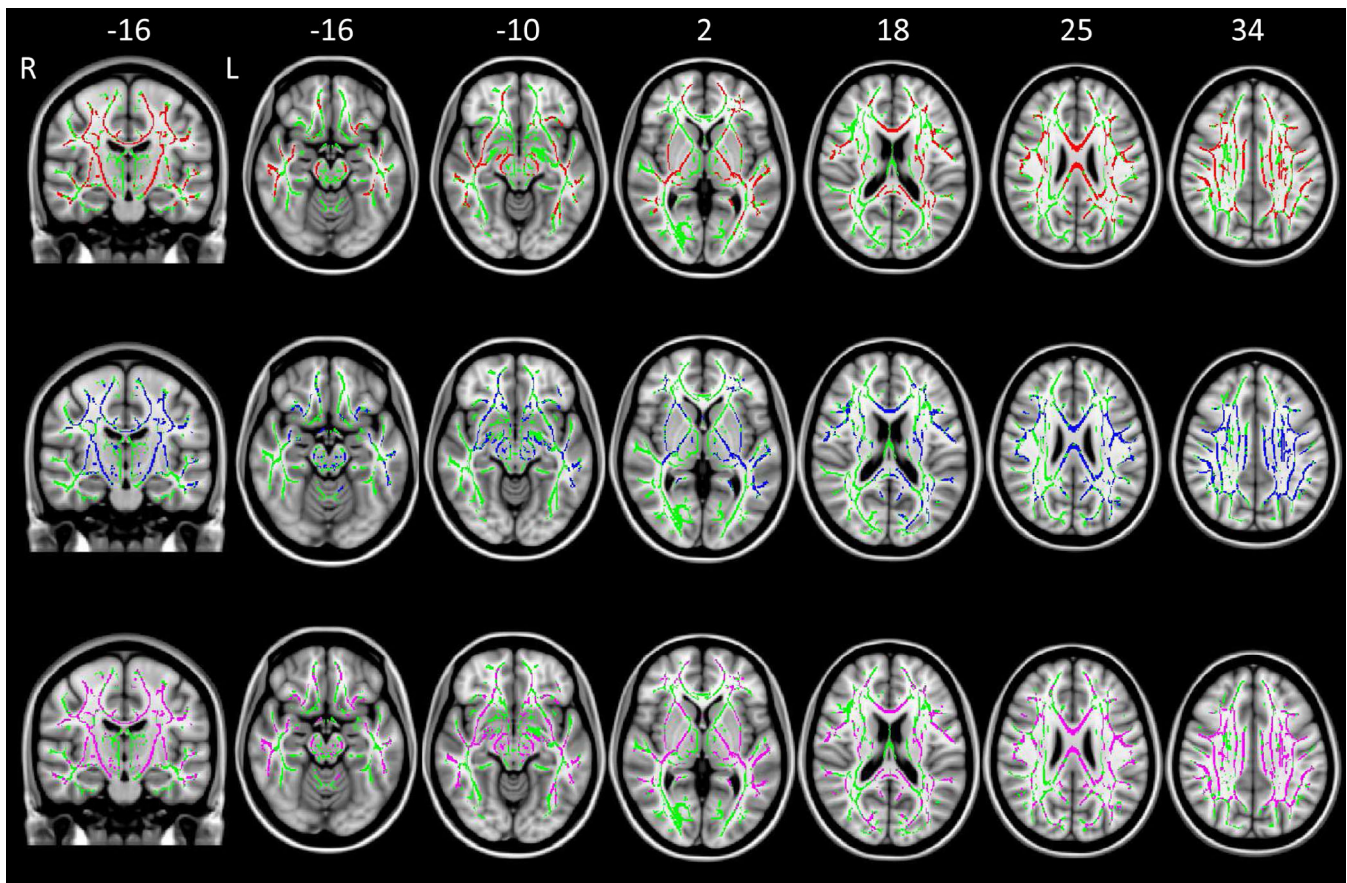


**FIGURE 2** TBSS results of comparison between classic ALS and KD patients. Axial and coronal T1-weighted images of the Montreal Neurologic Institute standard brain show tract-based spatial statistics results in patients with classic ALS compared with KD subjects. Voxel-wise group differences in fractional anisotropy (red), mean diffusivity (blue), axial diffusivity (orange), and radial diffusivity (purple) are shown. Results were overlaid on white-matter skeleton images (green;  $p < .05$ , corrected for multiple comparisons). Abbreviations. ALS: amyotrophic lateral sclerosis; KD: Kennedy's disease; L: left; R: right [Color figure can be viewed at [wileyonlinelibrary.com](http://wileyonlinelibrary.com)]

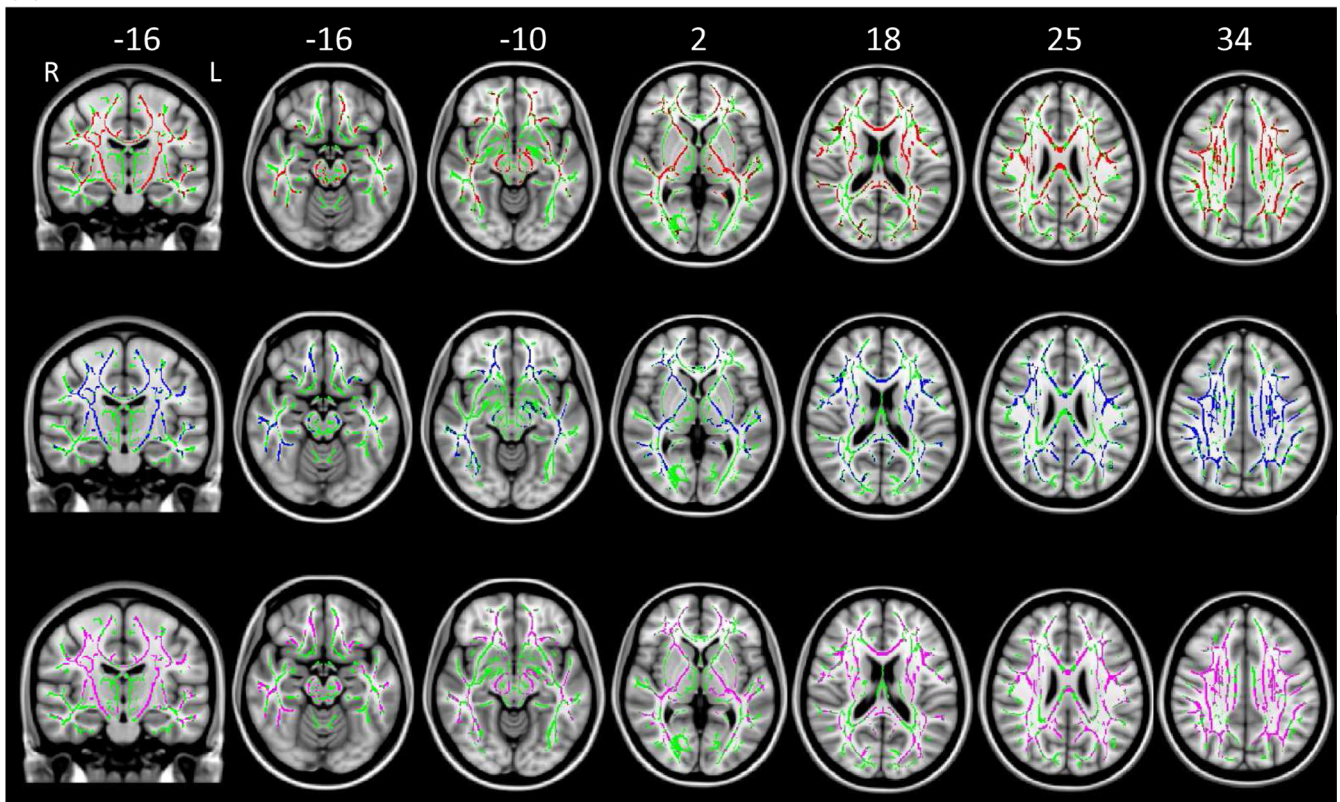
applied and the shorter disease duration of our cohort, as mentioned above. The present results showing no significant GM atrophy in LMND patients replicate previous findings from a smaller cohort (Spinelli et al., 2016), whereas the absence of GM reductions in ALS patients (using FDR correction and adjusting for age) differs from previous studies (Agosta et al., 2016; Chio et al., 2014; Spinelli et al., 2016). However, ALS patients of this cohort were selected to match KD patients for disease severity, as measured by ALSFRS-R scale. Therefore, only patients with a relatively mild disease were included, and the lack of detectable GM alterations using a conservative statistical threshold likely mirrors the level of functional impairment of these patients.

We found mild, nonclassifiable cognitive impairment in 16% of cognitively impaired KD patients, in keeping with previous studies describing subtle frontal lobe dysfunction and subclinical frontotemporal cognitive alterations during the course of the disease (Kasper et al., 2014; Soukup et al., 2009). Of note, behavioral changes were the most common symptoms in our KD cohort, being present in 36% of patients, including all those with cognitive impairment. To our knowledge, very few studies have investigated

cognition and behavior in KD. One of these reports described the case of a patient showing altered social conduct, forgetfulness, and a personality disorder, suggesting that behavioral alterations might be part of the disease clinical picture (Mirowska-Guzel, Seniow, Sulek, Lesniak, & Czlonkowska, 2009). More recently, a larger study reported significant impairment of social cognition in KD patients, particularly in tasks assessing empathy (Di Rosa et al., 2015). Our findings strengthen the importance of these reports, suggesting that behavioral alterations should be assessed in KD patients. Our results are also in line with previous observations of various degree of cognitive and behavioral alterations across other MND phenotypes, including LMND (Phukan et al., 2012; Raaphorst et al., 2011; Spinelli et al., 2016). However, the absence of significant differences from healthy controls indicated by structural MRI analysis in KD and LMND-slow patients of the present study suggests that neuroanatomical correlates of cognitive and behavioral impairment in these slow-progressing MND presentations should be sought in either functional rearrangements or very subtle structural alterations, not detectable using the techniques here applied.



(a)



(b)

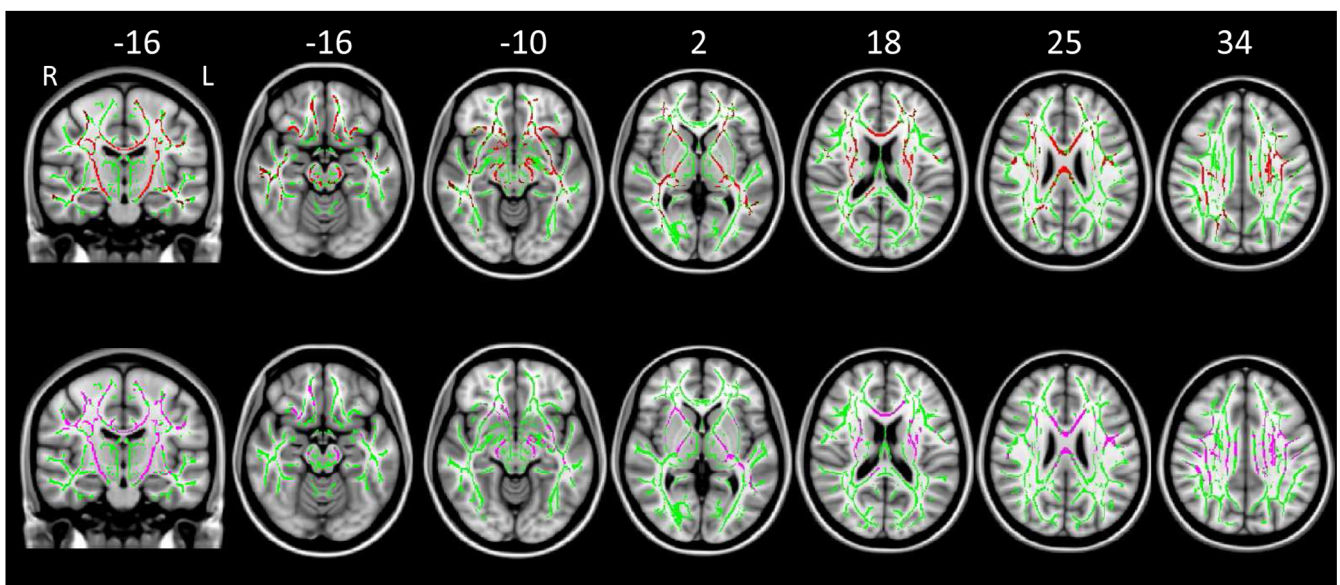


**FIGURE 3** TBSS results of comparison between classic ALS and LMND (fast and slow) patients. Axial and coronal T1-weighted images of the Montreal neurologic institute standard brain show tract-based spatial statistics results in patients with classic ALS compared with (a) LMND-fast and (b) LMND-slow patients. Voxel-wise group differences in fractional anisotropy (red), mean diffusivity (blue), and radial diffusivity (purple) are shown. Results were overlaid on white-matter skeleton images (green;  $p < .05$ , corrected for multiple comparisons). Abbreviations. ALS: amyotrophic lateral sclerosis; L: left; LMND: lower motor neuron disease; R: right [Color figure can be viewed at [wileyonlinelibrary.com](http://wileyonlinelibrary.com)]

The present study is not without limitations. First, this is a structural MRI study investigating GM and WM changes, while brain functional alterations have not been addressed. In fact, previous studies have

reported reduced prefrontal activation during executive tasks in LMND (Raaphorst et al., 2014), suggesting that functional MRI can provide additional insights into neuroanatomical alterations occurring during the



**TABLE 3** DT MRI metrics of corticospinal tracts in healthy controls and patients with KD, classic ALS, and LMND

		HC	KD	ALS	LMND-fast	LMND-slow	p*	Bp <sup>§</sup>
FA	L	0.53 ± 0.03	0.53 ± 0.03	0.51 ± 0.04	0.53 ± 0.03	0.53 ± 0.02	.13	.12
	R	0.53 ± 0.02	0.53 ± 0.03	0.52 ± 0.04	0.53 ± 0.03	0.53 ± 0.02	.18	.18
MD (×10 <sup>-3</sup> mm <sup>2</sup> s <sup>-1</sup> )	L	0.77 ± 0.04	0.77 ± 0.06	0.82 ± 0.08	0.79 ± 0.05	0.77 ± 0.04	.11	.11
	R	0.77 ± 0.04 <sup>a,b</sup>	0.78 ± 0.05	0.82 ± 0.07 <sup>c</sup>	0.81 ± 0.05 <sup>c</sup>	0.79 ± 0.05	.04	.04
axD (×10 <sup>-3</sup> mm <sup>2</sup> s <sup>-1</sup> )	L	1.25 ± 0.07	1.27 ± 0.08	1.31 ± 0.10	1.29 ± 0.08	1.27 ± 0.05	.31	.32
	R	1.28 ± 0.07	1.27 ± 0.05	1.32 ± 0.09	1.32 ± 0.07	1.29 ± 0.06	.20	.21
radD (×10 <sup>-3</sup> mm <sup>2</sup> s <sup>-1</sup> )	L	0.52 ± 0.05	0.52 ± 0.06	0.57 ± 0.08	0.54 ± 0.04	0.52 ± 0.04	.10	.08
	R	0.52 ± 0.04 <sup>a</sup>	0.53 ± 0.06	0.57 ± 0.07 <sup>b</sup>	0.55 ± 0.05 <sup>b</sup>	0.53 ± 0.05	.03	.02

Values are means ± standard deviations. \*p values refer to the between-group variance (F-values) from false discovery rate-corrected ANCOVA models adjusted for subjects' age and sex, followed by posthoc pairwise comparisons. a = p < .05 vs. ALS; b = p < .05 vs. LMND-fast; c = p < .05 vs. HC; <sup>§</sup>Bp: bootstrapped p values (i.e., the proportion of resampled F-values that are greater than the observed F-values) after 1,000 resamples, according to Westfall & Young (1993). Abbreviations. axD = axial diffusivity; ALS = Amyotrophic lateral sclerosis; FA = fractional anisotropy; HC = healthy controls; KD = Kennedy's disease; LMND = lower motor neuron-predominant disease; MD = mean diffusivity; radD = radial diffusivity.

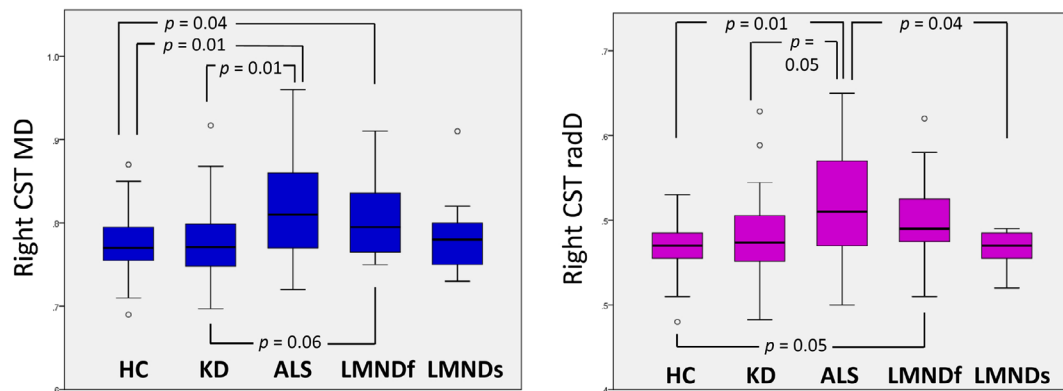


**FIGURE 4** DT MRI metrics of the CST in healthy controls, classic ALS and LMND patients. Mean diffusivity and radial diffusivity values of the corticospinal tracts of healthy controls and patient groups are plotted. Abbreviations. ALS: amyotrophic lateral sclerosis; CST: corticospinal tract; KD: Kennedy's disease; L: left; LMNDf: fast-progressing lower motor neuron disease; LMNDs: slow-progressing lower motor neuron disease; MD: mean diffusivity; radD: radial diffusivity; R: right [Color figure can be viewed at [wileyonlinelibrary.com](http://wileyonlinelibrary.com)]

disease course. Another limitation deals with the cross-sectional nature of the study. In this context, longitudinal studies are warranted in order to explore the progressive evolution of brain damage in KD.

In conclusion, the results of this multiparametric study—which is the first investigating the extent of CNS involvement in KD relative to other MND phenotypes—support the importance of a comprehensive cognitive and behavioral assessment even in rare LMN-predominant presentations, as well as the role of DT MRI as a promising diagnostic tool to be applied in the clinical setting to distinguish slow and fast-progressing MND.

## ACKNOWLEDGMENTS

The authors thank the patients and their families for the time and effort they dedicated to the research.

## CONFLICT OF INTEREST

E.G. Spinelli, P.M. Ferraro, G. Querin, N. Riva, C. Bertolin, I. Martinelli, C. Lunetta, A. Fontana, and G. Sorarù report no disclosures. F. Agosta

is Section Editor of *NeuroImage: Clinical*; has received speaker honoraria from Biogen Idec and Novartis; and receives or has received research supports from the Italian Ministry of Health, AriSLA (Fondazione Italiana di Ricerca per la SLA), and the European Research Council. M. Filippi is Editor-in-Chief of the *Journal of Neurology*; received compensation for consulting services and/or speaking activities from Biogen Idec, Merck-Serono, Novartis, Teva Pharmaceutical Industries; and receives research support from Biogen Idec, Merck-Serono, Novartis, Teva Pharmaceutical Industries, Roche, Italian Ministry of Health, Fondazione Italiana Sclerosi Multipla, and ARISLA (Fondazione Italiana di Ricerca per la SLA).

## AUTHOR CONTRIBUTIONS

M.F. coordinated the study. E.G.S., F.A., G.S., and M.F. were responsible for study conception and design. E.G.S., F.A., P.M.F., G.Q., N.R., C.B., I.M., C.L., A.F., and G.S. were responsible for acquisition and analyses of data. All authors were responsible for drafting or revising the text.

## ORCID

Massimo Filippi  <https://orcid.org/0000-0002-5485-0479>

## REFERENCES

- Agosta, F., Ferraro, P. M., Riva, N., Spinelli, E. G., Chio, A., Canu, E., ... Filippi, M. (2016). Structural brain correlates of cognitive and behavioral impairment in MND. *Human Brain Mapping, 37*(4), 1614–1626. <https://doi.org/10.1002/hbm.23124>
- Agosta, F., Galantucci, S., Canu, E., Cappa, S. F., Magnani, G., Franceschi, M., ... Filippi, M. (2013). Disruption of structural connectivity along the dorsal and ventral language pathways in patients with nonfluent and semantic variant primary progressive aphasia: A DT MRI study and a literature review. *Brain and Language, 127*(2), 157–166. <https://doi.org/10.1016/j.bandl.2013.06.003>
- Agosta, F., Galantucci, S., Riva, N., Chio, A., Messina, S., Iannaccone, S., ... Filippi, M. (2014). Intrahemispheric and interhemispheric structural network abnormalities in PLS and ALS. *Human Brain Mapping, 35*(4), 1710–1722. <https://doi.org/10.1002/hbm.22286>
- Alberici, A., Geroldi, C., Cotelli, M., Adorni, A., Calabria, M., Rossi, G., ... Kertesz, A. (2007). The frontal behavioural inventory (Italian version) differentiates frontotemporal lobar degeneration variants from Alzheimer's disease. *Neurological Sciences, 28*(2), 80–86. <https://doi.org/10.1007/s10072-007-0791-3>
- Basso, A., Capitani, E., & Laiacona, M. (1987). Raven's coloured progressive matrices: Normative values on 305 adult normal controls. *Functional Neurology, 2*(2), 189–194.
- Behrens, T. E., Berg, H. J., Jbabdi, S., Rushworth, M. F., & Woolrich, M. W. (2007). Probabilistic diffusion tractography with multiple fibre orientations: What can we gain? *NeuroImage, 34*(1), 144–155. <https://doi.org/10.1016/j.neuroimage.2006.09.018>
- Brooks, B. R., Miller, R. G., Swash, M., Munsat, T. L., & World Federation of Neurology Research Group on Motor Neuron Diseases. (2000). El Escorial revisited: Revised criteria for the diagnosis of amyotrophic lateral sclerosis. *Amyotrophic Lateral Sclerosis and Other Motor Neuron Disorders, 1*(5), 293–299.
- Carlesimo, G. A., Caltagirone, C., & Gainotti, G. (1996). The mental deterioration battery: Normative data, diagnostic reliability and qualitative analyses of cognitive impairment. The Group for the Standardization of the mental deterioration battery. *European Neurology, 36*(6), 378–384.
- Chahin, N., Klein, C., Mandrekar, J., & Sorenson, E. (2008). Natural history of spinal-bulbar muscular atrophy. *Neurology, 70*(21), 1967–1971. <https://doi.org/10.1212/01.wnl.0000312510.49768.eb>
- Chio, A., Calvo, A., Moglia, C., Mazzini, L., Mora, G., & Group, P. S. (2011). Phenotypic heterogeneity of amyotrophic lateral sclerosis: A population based study. *Journal of Neurology, Neurosurgery, and Psychiatry, 82*(7), 740–746. <https://doi.org/10.1136/jnnp.2010.235952>
- Chio, A., Pagani, M., Agosta, F., Calvo, A., Cistaro, A., & Filippi, M. (2014). Neuroimaging in amyotrophic lateral sclerosis: Insights into structural and functional changes. *Lancet Neurology, 13*(12), 1228–1240. [https://doi.org/10.1016/S1474-4422\(14\)70167-X](https://doi.org/10.1016/S1474-4422(14)70167-X)
- Ciccarelli, O., Behrens, T. E., Altmann, D. R., Orrell, R. W., Howard, R. S., Johansen-Berg, H., ... Thompson, A. J. (2006). Probabilistic diffusion tractography: A potential tool to assess the rate of disease progression in amyotrophic lateral sclerosis. *Brain, 129*(Pt 7), 1859–1871. <https://doi.org/10.1093/brain/awl100>
- Dale, A. M., Fischl, B., & Sereno, M. I. (1999). Cortical surface-based analysis. I. Segmentation and surface reconstruction. *NeuroImage, 9*(2), 179–194. <https://doi.org/10.1006/nimg.1998.0395>
- Della Sala, S., MacPherson, S. E., Phillips, L. H., Sacco, L., & Spinnler, H. (2003). How many camels are there in Italy? Cognitive estimates standardised on the Italian population. *Neurological Sciences, 24*(1), 10–15. <https://doi.org/10.1007/s100720300015>
- Di Rosa, E., Soraru, G., Kleinbub, J. R., Calvo, V., Vallesi, A., Querin, G., ... Palmieri, A. (2015). Theory of mind, empathy and neuropsychological functioning in X-linked spinal and bulbar muscular atrophy: A controlled study of 20 patients. *Journal of Neurology, 262*(2), 394–401. <https://doi.org/10.1007/s00415-014-7567-5>
- Finsterer, J. (2010). Perspectives of Kennedy's disease. *Journal of the Neurological Sciences, 298*(1–2), 1–10. <https://doi.org/10.1016/j.jns.2010.08.025>
- Folstein, M. F., Folstein, S. E., & McHugh, P. R. (1975). "mini-mental state". A practical method for grading the cognitive state of patients for the clinician. *Journal of Psychiatric Research, 12*(3), 189–198.
- Galantucci, S., Tartaglia, M. C., Wilson, S. M., Henry, M. L., Filippi, M., Agosta, F., ... Gorno-Tempini, M. L. (2011). White matter damage in primary progressive aphasia: A diffusion tensor tractography study. *Brain, 134*(Pt 10), 3011–3029. doi:awr099 [pii]10.1093/Brain/awr099.
- Garaci, F., Toschi, N., Lanzafame, S., Marfia, G. A., Marziali, S., Meschini, A., ... Floris, R. (2015). Brain MR diffusion tensor imaging in Kennedy's disease. *The Neuroradiology Journal, 28*(2), 126–132. <https://doi.org/10.1177/1971400915581740>
- Grunseich, C., Rinaldi, C., & Fischbeck, K. H. (2014). Spinal and bulbar muscular atrophy: Pathogenesis and clinical management. *Oral Diseases, 20*(1), 6–9. <https://doi.org/10.1111/odi.12121>
- Hamilton, M. (1960). A rating scale for depression. *Journal of Neurology, Neurosurgery, and Psychiatry, 23*, 56–62.
- Horsfield, M. A. (1999). Mapping eddy current induced fields for the correction of diffusion-weighted echo planar images. *Magnetic Resonance Imaging, 17*(9), 1335–1345.
- Kasper, E., Wegryzn, M., Marx, I., Korp, C., Kress, W., Benecke, R., ... Prudlo, J. (2014). Minor cognitive disturbances in X-linked spinal and bulbar muscular atrophy, Kennedy's disease. *Amyotroph Lateral Scler Frontotemporal Degener, 15*(1–2), 15–20. <https://doi.org/10.3109/21678421.2013.837927>
- Kassubek, J., Juengling, F. D., & Sperfeld, A. D. (2007). Widespread white matter changes in Kennedy disease: A voxel based morphometry study. *Journal of Neurology, Neurosurgery, and Psychiatry, 78*(11), 1209–1212. <https://doi.org/10.1136/jnnp.2006.112532>
- La Spada, A. R., Wilson, E. M., Lubahn, D. B., Harding, A. E., & Fischbeck, K. H. (1991). Androgen receptor gene mutations in X-linked spinal and bulbar muscular atrophy. *Nature, 352*(6330), 77–79. <https://doi.org/10.1038/352077a0>
- Laiacona, M., Inzaghi, M. G., De Tanti, A., & Capitani, E. (2000). Wisconsin card sorting test: A new global score, with Italian norms, and its relationship with the Weigl sorting test. *Neurological Sciences, 21*(5), 279–291.
- Lee, J. H., Shin, J. H., Park, K. P., Kim, I. J., Kim, C. M., Lim, J. G., ... Kim, D. S. (2005). Phenotypic variability in Kennedy's disease: Implication of the early diagnostic features. *Acta Neurologica Scandinavica, 112*(1), 57–63. <https://doi.org/10.1111/j.1600-0404.2005.00428.x>
- Miceli, G., Laudanna, A., Burani, C., & Capasso, R. (1994). *Batteria per l'Analisi del Deficit Afasico*. B.A.D.A. [B.A.D.A. A Battery for the Assessment of Aphasic Disorders. Roma: CEPSAG.
- Mirowska-Guzel, D., Seniow, J., Sulek, A., Lesniak, M., & Czlonkowska, A. (2009). Are cognitive and behavioural deficits a part of the clinical picture in Kennedy's disease? A case study. *Neurocase, 15*(4), 332–337. <https://doi.org/10.1080/13554790902842003>
- Monaco, M., Costa, A., Caltagirone, C., & Carlesimo, G. A. (2013). Forward and backward span for verbal and visuo-spatial data: Standardization and normative data from an Italian adult population. *Neurological Sciences, 34*(5), 749–754. <https://doi.org/10.1007/s10072-012-1130-x>
- Muller, H. P., Agosta, F., Riva, N., Spinelli, E. G., Comi, G., Ludolph, A. C., ... Kassubek, J. (2018). Fast progressive lower motor neuron disease is an ALS variant: A two-Centre tract of interest-based MRI data analysis. *NeuroImage Clin, 17*, 145–152. <https://doi.org/10.1016/j.nicl.2017.10.008>

- Nichols, T. E., & Holmes, A. P. (2002). Nonparametric permutation tests for functional neuroimaging: A primer with examples. *Human Brain Mapping, 15*(1), 1–25.
- Novelli, G., Papagno, C., Capitani, E., Laiacona, M., Vallar, G., & Cappa, S. (1986). Tre test clinici di ricerca e produzione lessicale. Taratura su soggetti normali. *Archivio di Psicologia, Neurologia e Psichiatria, 47*(4), 477–506.
- Orsini, A., Grossi, D., Capitani, E., Laiacona, M., Papagno, C., & Vallar, G. (1987). Verbal and spatial immediate memory span: Normative data from 1355 adults and 1112 children. *Italian Journal of Neurological Sciences, 8*(6), 539–548.
- Phukan, J., Elamin, M., Bede, P., Jordan, N., Gallagher, L., Byrne, S., ... Hardiman, O. (2012). The syndrome of cognitive impairment in amyotrophic lateral sclerosis: A population-based study. *Journal of Neurology, Neurosurgery, and Psychiatry, 83*(1), 102–108. <https://doi.org/10.1136/jnnp-2011-300188>
- Pieper, C. C., Konrad, C., Sommer, J., Teismann, I., & Schiffbauer, H. (2013). Structural changes of central white matter tracts in Kennedy's disease—A diffusion tensor imaging and voxel-based morphometry study. *Acta Neurologica Scandinavica, 127*(5), 323–328. <https://doi.org/10.1111/ane.12018>
- Raaphorst, J., Beeldman, E., Schmand, B., Berkhout, J., Linssen, W. H., van den Berg, L. H., ... de Haan, R. J. (2012). The ALS-FTD-Q: A new screening tool for behavioral disturbances in ALS. *Neurology, 79*(13), 1377–1383. <https://doi.org/10.1212/WNL.0b013e31826c1aa1>
- Raaphorst, J., de Visser, M., van Tol, M. J., Linssen, W. H., van der Kooi, A. J., de Haan, R. J., ... Schmand, B. (2011). Cognitive dysfunction in lower motor neuron disease: Executive and memory deficits in progressive muscular atrophy. *Journal of Neurology, Neurosurgery, and Psychiatry, 82*(2), 170–175. <https://doi.org/10.1136/jnnp.2009.204446>
- Raaphorst, J., van Tol, M. J., Groot, P. F., Altena, E., van der Werf, Y. D., Majoie, C. B., ... Veltman, D. J. (2014). Prefrontal involvement related to cognitive impairment in progressive muscular atrophy. *Neurology, 83*(9), 818–825. <https://doi.org/10.1212/WNL.0000000000000745>
- Rhodes, L. E., Freeman, B. K., Auh, S., Kokkinis, A. D., La Pean, A., Chen, C., ... Fischbeck, K. H. (2009). Clinical features of spinal and bulbar muscular atrophy. *Brain, 132*(Pt 12), 3242–3251. <https://doi.org/10.1093/brain/awp258>
- Rosenbohm, A., Muller, H. P., Hubers, A., Ludolph, A. C., & Kassubek, J. (2016). Corticoefferent pathways in pure lower motor neuron disease: A diffusion tensor imaging study. *Journal of Neurology, 263*(12), 2430–2437. <https://doi.org/10.1007/s00415-016-8281-2>
- Smith, S. M., & Nichols, T. E. (2009). Threshold-free cluster enhancement: Addressing problems of smoothing, threshold dependence and localisation in cluster inference. *NeuroImage, 44*(1), 83–98. <https://doi.org/10.1016/j.neuroimage.2008.03.061>
- Soukup, G. R., Sperfeld, A. D., Uttner, I., Karitzky, J., Ludolph, A. C., Kassubek, J., & Schreiber, H. (2009). Frontotemporal cognitive function in X-linked spinal and bulbar muscular atrophy (SBMA): A controlled neuropsychological study of 20 patients. *Journal of Neurology, 256*(11), 1869–1875. <https://doi.org/10.1007/s00415-009-5212-5>
- Spinelli, E. G., Agosta, F., Ferraro, P. M., Riva, N., Lunetta, C., Falzone, Y. M., ... Filippi, M. (2016). Brain MR imaging in patients with lower motor neuron-predominant disease. *Radiology, 280*(2), 545–556. <https://doi.org/10.1148/radiol.2016151846>
- Strong, M. J., Abrahams, S., Goldstein, L. H., Woolley, S., McLaughlin, P., Snowden, J., ... Turner, M. R. (2017). Amyotrophic lateral sclerosis—Frontotemporal spectrum disorder (ALS-FTSD): Revised diagnostic criteria. *Amyotroph Lateral Scler Frontotemporal Degener, 18*(3–4), 153–174. <https://doi.org/10.1080/21678421.2016.1267768>
- Unrath, A., Muller, H. P., Riecker, A., Ludolph, A. C., Sperfeld, A. D., & Kassubek, J. (2010). Whole brain-based analysis of regional white matter tract alterations in rare motor neuron diseases by diffusion tensor imaging. *Human Brain Mapping, 31*(11), 1727–1740. <https://doi.org/10.1002/hbm.20971>
- van den Berg-Vos, R. M., Visser, J., Franssen, H., de Visser, M., de Jong, J. M., Kalmijn, S., ... van den Berg, L. H. (2003). Sporadic lower motor neuron disease with adult onset: Classification of subtypes. *Brain, 126*(Pt 5), 1036–1047.
- Weigl, E. (1927). On the psychology of so-called processes of abstraction. *Zeitschrift für Psychologie, 103*, 245–300.
- Westfall, P. H., & Young, S. S. (1993). Resampling-based multiple testing: Examples and methods for p-value adjustment. *Technometrics, 35*, 450–451.

## SUPPORTING INFORMATION

Additional supporting information may be found online in the Supporting Information section at the end of this article.

**How to cite this article:** Spinelli EG, Agosta F, Ferraro PM, et al. Brain MRI shows white matter sparing in Kennedy's disease and slow-progressing lower motor neuron disease. *Hum Brain Mapp.* 2019;40:3102–3112. <https://doi.org/10.1002/hbm.24583>